Statistical Thermodynamics of Polymer Aggregates in Solution: Modeling of Single Polymer Dispersion Particles†

Olaf A. Evers,*,‡ Gregor Ley,§ and Erich Hädicke§

Zentrale Informatik and Kunststofflaboratorium, BASF Aktiengesellschaft, D-6700 Ludwigshafen am Rhein, FRG

Received October 1, 1992; Revised Manuscript Received March 2, 1993

ABSTRACT: The self-consistent mean-field theory of Scheutjens and Fleer for a spherical lattice is applied to model aggregates of homopolymers with and without lyophilic groups in solution. Information can be obtained on the spatial distribution of the individual chain segments without making artificial assumptions on the position of any chain segment in the aggregate. Details of the inner and surface fine structure of dispersed polymer particles and its dependence on particle size, molecular weight (distribution), polymer structure, and solvent quality are studied. For homopolymers it is found that the segments at the chain ends are preferentially located at the exterior side of the polymer/solution interface. The presence of lyophilic groups at the ends of the chain enhances the accumulation of chain ends at the surface. For polydisperse samples the interfacial region contains a higher fraction of short chains than the interior of the particle. Mixtures containing homopolymers with one, two, and no lyophilic end groups form aggregates in which a clear segregation of these chain types is found. The distribution of end segments and shorter chains in the particles may be an important parameter in latex particle film formation.

I. Introduction

A number of experimental[1-4] studies on the interdiffusion of chains during the process of latex film formation have been published in the last five years. From small-angle neutron scattering (SANS) experiments Hahn et al.[1,2] showed that massive interdiffusion of polymer chains between particles takes place during coalescence of *n*-butyl methacrylate copolymer latex particles. They determined the radius of gyration during film formation of a small number of deuterated latex particles mixed with undeuterated particles. Linné et al.[3] did similar experiments on polystyrene latex particles. Yoo et al.[4] correlated SANS experiments with tensile strength measurements during film formaton of high molecular polystyrene latex particles. They found that the minimum penetration depth for full tensile strength is at least 30–35 Å, comparable to the radius of gyration of the critical entanglement molecular weight for polystyrene. Since the emulsion polymerization reaction for high molecular polystyrene produces a polymer chain with sulfate ion chain ends, Yoo et al. assumed that these chain ends are predominantly anchored at the latex particle–water interface. Conductometric titration of polystyrene latex particles by van den Hul and Vanderhoff[5] showed that most of the sulfate and hydroxyl end groups are found on the particle surface. However, in some of their samples up to 55% of the end groups were buried inside the particle. According to de Gennes[6,7] reptation model chain ends play an important role for chain diffusion. Therefore, Yoo et al. proposed the hypothesis that the minimum penetration depth for full tensile strength development depends not so much on molecular weight but on the chain end distribution within the particle. Information on the orientation of the chains in latex particles depending on whether or not one or more lyophilic groups are present in the chains would be helpful for the interpretation of experimental results on film formation of latex particles.

Monte Carlo[8,9] studies and molecular dynamics simulations[10] have been reported on planar polymer films confined between two parallel surfaces. It is found that the chains next to the surface tend to arrange themselves with their longest spatial dimension parallel to the film. A Monte Carlo study on the polymer–vacuum interface has been reported by Madden.[11] A planar polydisperse polymer fim was adsorbed on a planar flat surface to fix the slab and on the other side exposed to vacuum. It appears from this study that the chain ends near the surface tend to favor the exterior (low-density) side. Also it is found that the shorter chains are depleted from the melt toward the vacuum. A statistical thermodynamic approach to the planar polymer–vacuum interface of a monodisperse polymer film based on the mean-field lattice model of Scheutjens and Fleer[12-14] has recently been presented by Theodorou.[15] In accordance with the Monte Carlo results of Madden,[11] the chain ends are found to preferentially concentrate at the exterior side of the surface, whereas the middle segments are depleted from the interfacial region.

In this paper the self-consistent mean-field theory of Scheutjens and Fleer[12-14] is used to describe the association of nonionic polymer chains into spherical particles. We will use the multicomponent extension of Evers et al.[16] and the spherical lattice as it has been used by van Lent and Scheutjens[17] to model block copolymer micelles. The theory of Scheutjens and Fleer[12-14] is based on a lattice model to achieve a finite number of different conformations of the molecules. In contrast to a similar mean-field lattice theory of Marqusee and Dill[18] for planar and spherical aggregates, the model of Scheutjens and Fleer makes no a priori assumptions about the conformations of the chains in the lattice. All possible conformations of the chains on the spherical lattice are evaluated using a self-consistent method. The energetic interactions are accounted for by a mean-field Flory–Huggins type approach. By applying the Scheutjens and Fleer theory to spherical aggregates of polymers, it is possible, as has been done by Theodorou[15] for planar polymer films, to obtain detailed information on the position of every chain segment in the lattice.

After a brief review of the extended Scheutjens and Fleer model, systematic numerical results are presented for spherical aggregates of monodisperse and polydisperse homopolymers and the effect of the presence of lyophilic groups in the chain. The structure of the modeled single polymer dispersion particles will be analyzed depending

† This paper is dedicated to the memory of Dr. Jan Scheutjens.
‡ Zentrale Informatik, BASF Aktiengesellschaft.
§ Kunststofflaboratorium, BASF Aktiengesellschaft.

0024-9297/93/2226-2885$04.00/0

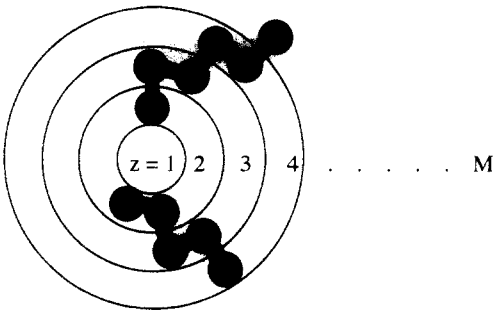

Figure 1. Cross section of a spherical lattice showing the definition of the lattice layers as is used to model spherical aggregates.

on the Flory–Huggins interaction parameters between lyophobic segments, lyophilic segments, solvent molecules, chain length, and polydispersity. Especially the fine structure and the extent of the interfacial region and its consequences on the application of dispersions is discussed.

II. Model

In this section we briefly discuss the model of Scheutjens and Fleer[12-14] in the multicomponent version of Evers et al.[16] using a spherical lattice as has been used by van Lent and Scheutjens[17] to model diblock copolymer micelles. For a detailed derivation of the theory the reader is referred to the original paper of Evers et al.[16]

Spherical Lattice. The self-consistent mean-field theory of Scheutjens and Fleer is based on a lattice model. In a lattice the number of possible conformations the chains can adopt is finite. The basic disadvantage is first the assumption of an equal volume for the different types of segments present in the system and second the restriction on the conformational space of the chains. To model a polymer aggregate, we use a lattice with spherical geometry. A cross section is shown in Figure 1. We assume all lattice sites to be occupied. The lattice sites are grouped into shells, the layers. These layers are numbered sequentially, starting with layer $z = 1$ at the center of the lattice to the outermost solvent layer M. At the outer surface of layer M a reflecting boundary condition is applied.

A mean-field approximation is applied within each shell or layer. Therefore, only inhomogeneities in one dimension, i.e, in the direction perpendicular to the shells, are taken into account. As a consequence of this mean-field approximation the aggregates cannot find the optimal geometry by themselves; they rather have to accept the imposed symmetrical spherical geometry of the lattice. As van Lent and Scheutjens[18] have discussed in the application of this spherical lattice to block copolymer micelles, three conditions must hold:

1. All lattice sites have equal volume.
2. All lattice layers are equidistant.
3. The coordination number Z, i.e., the number of nearest-neighbor sites of a single lattice site, is constant throughout the lattice.

To fulfill these conditions, the lattice sites will have different shapes depending on the distance to the center, i.e., zl_0, where l_0 is the layer thickness. The volume of a lattice layer is denoted by $L(z)$ and is simply given by

$$L(z) = \frac{4}{3}\pi(z^3 - (z-1)^3)l_0^3 \tag{1}$$

In a lattice with planar geometry the a priori probability λ_1 to make a random-walk step from one layer to an adjacent layer is given by the fraction of nearest neighbors a site has in one of the two adjacent layers. Thus, for a hexagonal lattice $\lambda_1 = {}^3/_{12}$ and the transition probability λ_0 to make a step in the same layer is in that case $\lambda_0 = {}^6/_{12}$. Of course, $\lambda_1 + \lambda_0 + \lambda_1$ must equal 1. In a spherical lattice the a priori transition probabilities $\lambda(z+1|z)$ for a random-walk step from layer z to layer $z + 1$ will depend on z. Let us derive the expression for $\lambda(z+1|z)$.

The sum of all transition probabilities for a step starting from layer z should equal 1.

$$\lambda(z+1|z) + \lambda(z|z) + \lambda(z-1|z) = 1 \tag{2}$$

For a random walk on a lattice it should make no difference whether we start on layer z and make one step to layer $z + 1$ or vice versa. The a priori probability to place a segment on an empty lattice in layer z equals $L(z)/V$, where V is the volume of the total system. The probability to place the next segment in layer $z + 1$, given that the first segment is in layer z, is then $\lambda(z+1|z)\,L(z)/V$. This should equal the probability of the opposite placements (segment 1 in layer $z + 1$ and segment 2 in layer z).

$$\lambda(z+1|z)\,L(z) = \lambda(z|z+1)\,L(z+1) \tag{3}$$

In the limit that $z \to \infty$, $\lambda(z+1|z)$ should equal λ_1 of a planar lattice:

$$\lim_{z\to\infty} \lambda(z+1|z) = \lambda_1 \tag{4}$$

The outer surface area of layer z is denoted by $S(z)$ and is given by

$$S(z) = 4\pi z^2 l_0^2 \tag{5}$$

The ratio of the transition probabilities, $\lambda(z+1|z)$ and $\lambda(z-1|z)$ respectively should be proportional to the ratio of the outer and inner surface areas of layer z.

$$\frac{\lambda(z+1|z)}{\lambda(z-1|z)} = \frac{S(z)}{S(z-1)} \tag{6}$$

By substituting eq 6 into eq 3, we obtain

$$\frac{\lambda(z|z+1)}{\lambda(z-1|z)} = \frac{S(z)}{L(z+1)}\frac{L(z)}{S(z-1)} \tag{7}$$

Realizing that the a priori transition probabilities for a step from layer $z + 1$ to layer z can not depend on the outer surface area of layer $z - 1$ and also not on the transition probability $\lambda(z-1|z)$, we derive with the help of eq 4 the final expressions for the transition probabilities:

$$\lambda(z-1|z) = \lambda_1\frac{S(z-1)l_0}{L(z)}$$

$$\lambda(z,z) = 1 - \lambda(z-1|z) - \lambda(z+1|z) \tag{8}$$

$$\lambda(z+1|z) = \lambda_1\frac{S(z)l_0}{L(z)}$$

Segment Density Distribution. If polymer chains are poorly soluble in the medium, they will aggregate. In the mixture a density gradient is then found due to the unfavorable contacts between the polymer segments and the solvent molecules. To put it more general, every individual segment is subjected to a local potential which depends on its position in the lattice. In the spherical lattice the potential of a segment of type x in layer z is denoted by $u_x(z)$. This implies a mean-field approximation within each lattice layer, since inhomogeneities within each layer are neglected. If the potential profiles $\{u_x\}$, $\{u_y\}$, ... for the different segment types are known, the segment density profiles $\{\phi_x\}$, $\{\phi_y\}$, ..., being defined as the number

of segments of the same type per lattice site, can be calculated using Boltzmann statistics. The potential $u_x(z)$ can be derived from statistical thermodynamics[16]

$$u_x(z) = u'(z) + u_x^{\text{int}}(z) \tag{9}$$

The first term on the right-hand side of eq 9, namely, $u'(z)$, is independent of the type of segment; it ensures that every lattice site is filled. The parameter $u'(z)$ could be interpreted as a "hard-core potential". It has to be found self consistently from the boundary conditions $\sum_x \phi_x(z) = 1$, for every z. The second term, $u_x^{\text{int}}(z)$, is the result of energetic interactions between segment x in layer z and surrounding segments. For this interaction potential we will use the well-known Flory–Huggins interaction parameter χ_{xy}, defined as the energy change (in units of kT) associated with the transfer of a segment of type x from a solution of pure x to a solution of pure y. By definition $\chi_{xx} = 0$. On average, a segment in layer z has $\langle\phi_y(z)\rangle$ contacts with y-segments, where the contact fraction $\langle\phi_y(z)\rangle$ is given by

$$\langle\phi_y(z)\rangle = \lambda(z-1|z)\,\phi_y(z-1) + \lambda(z|z)\,\phi_y(z) + \lambda(z+1|z)\,\phi_y(z+1) \tag{10}$$

Thus, the potential $u_x^{\text{int}}(z)$ becomes

$$u_x^{\text{int}}(z) = kT\sum_y \chi_{xy}\langle\phi_y(z)\rangle \tag{11}$$

For a mixture of monomers, the segment density profiles can be calculated straightforward as $\phi_x(z) = C_x \exp[-u_x(z)/kT]$, where C_x is a normalization constant which will be discussed later. The Boltzmann factor $\exp[-u_x(z)/kT]$ is called the monomer weighting factor $g_x(z)$.

$$g_x(z) = \exp\left[-\frac{u_x(z)}{kT}\right] \tag{12}$$

and gives the probability to find a "free" monomer (not connected to other monomers) of type x in layer z.

For the segment density in layer z of a segment with ranking number s in a chain of type i, $\phi_i(z,s)$, we must account for the interconnection of the segments using Markov statistics. The Boltzmann factor for the conditional event of finding segment s of chains i in layer z is the result of three separate events:

(1) Segment s must be located in layer z.

(2) The chain part from segment 1 up to segment $s-1$ must have its last segment in an adjacent lattice site of segment s, thus, in one of the layers $z-1$, z, or $z+1$.

(3) The other chain part from segment $s+1$ up to the last segment, r_i, must have segment $s+1$ in one of the layers $z-1$, z, or $z+1$.

The weighting factor for the first event is given by $g_i(z,s)$. For instance, if segment s is of type x, $g_i(z,s)$ equals $g_x(z)$. For the second event we make use of the chain weighting factor $g_i(z,s|1)$, which gives the conditional probability to find segment s of the chain part from segment 1 up to segment s in layer z independent of the position of the other $s-1$ segments as long as they are connected. The chain weighting factor $g_i(z,s|r_i)$ is defined in the same way but for the chain part from segment s up to segment r_i. It is clear that $g_i(z,1|1) = g_i(z,1)$ and $g_i(z,r_i|r_i) = g_i(z,r_i)$. The chain weighting factor $g_i(z,s|1)$ can be derived from the chain weighting factor of the chain part from segment 1 up to segment $s-1$. If segment s is in layer z, then segment $s-1$ must be located in an adjacent lattice site in one of the layers $z-1$, z, or $z+1$. If we allow for backfolding, then $g_i(z,s|1)$ is given by

$$g_i(z,s|1) = g_i(z,s)\,\langle g_i(z,s-1|1)\rangle \tag{13}$$

where the average $\langle g_i(z,s|1)\rangle$ is defined in the same way as $\langle\phi_y(z)\rangle$ in eq 10. Equation 13 is a recurrency relation, valid for $s > 1$. For $g_i(z,s|r_i)$ we have a similar recurrency equation

$$g_i(z,s|r_i) = g_i(z,s)\,\langle g_i(z,s+1|r_i)\rangle \tag{14}$$

which applies for any $s < r_i$. Finally, multiplying the weighting factors of the three events gives the density in layer z of segment s of a chain of type i.

$$\phi_i(z,s) = C_i\frac{g_i(z,s|1)\,g_i(z,s|r_i)}{g_i(z,s)} \tag{15}$$

The segment density $\phi_i(z)$ of all segments belonging to chains of type i in layer z is given by the summation of $\phi_i(z,s)$ over all segments of the chain,

$$\phi_i(z) = \sum_{s=1}^{r_i}\phi_i(z,s) \tag{16}$$

The volume fraction $\phi_{xi}(z)$ due to segments of type x in layer z belonging to molecules of type i is obtained by performing the summation in eq 16 only over those segments s which are of type x. The total volume fraction $\phi_x(z)$ of all segments of type x in layer z is then obtained by summation of $\phi_{xi}(z)$ over all molecule types i.

The normalization constant C_i can be expressed in terms of the total number n_i of chains i in the system. The number of any segment s of chains i equals n_i; hence, $\sum_z L(z)\,\phi_i(z,s) = \sum_z L(z)\,\phi_i(z,r_i) = n_i$. Summing both sides of eq 15 for segment r_i over z, weighting with $L(z)$, and realizing that the right-hand side of eq 15 for r_i is nothing else than $g_i(z,r_i|1)$, we obtain

$$C_i = \frac{n_i}{\sum_z L(z)\,g_i(z,r_i|1)} \tag{17}$$

Numerical Aspects. From an initial guess for the monomer potentials $u_x(z)$ we can calculate the corresponding monomer weighting factors $g_x(z)$ according to eq 12 and the volume fraction distributions from eq 13–17. In turn, $u_x(z)$ can be calculated from the segment densities $\phi_x(z)$ and an initial guess for $u'(z)$ according to eqs 9–11. A numerical iteration procedure is used to obtain a self-consistent solution by the formulation of an implicit set of simultaneous equations as given in ref 16 under the condition $\sum_x \phi_x(z) = 1$ for all z. This set of simultaneous equations in the unknown variables $\{u_x\}$, $\{u_y\}$, ... can be solved using standard numerical techniques, for instance, with the FORTRAN program HYBRD of Powell. At BASF AG we use in-house software written in the computer language C.

The input parameters are the segment sequences for all the components in the system, the χ parameters between the various segment types, the total number of lattice layers M, and the total number of molecules n_i for all different types of molecules in the system.

III. Results and Discussion

In this section we first present numerical results on spherical aggregates of monodisperse homopolymers. Especially the average location of the individual segments of these homopolymer chains in the aggregates will be discussed depending on the particle size, the chain length, and the solvent quality. In the second part the effect of

polydispersity on homopolymer aggregates is presented. The presence of lyophilic groups (copolymers) on the orientation of the chains in the aggregates is discussed in the third and fourth part. All calculations are done on a hexagonal lattice ($\lambda_1 = {}^3/_{12}$) with a spherical geometry, and—if not otherwise indicated—a value of 1.0 has been used for the Flory–Huggins parameter χ between segment and solvent. The aggregates modeled in this study contain no stabilizing agents (surfactants). As van Lent and Scheutjens[17] have shown, one or two lyophilic groups at the chain ends of large polymers are not enough to stabilize the aggregates. Therefore, the polymer aggregates of the polymers in this study do not represent equilibrium structures since the Gibbs free energy can always be lowered by adding more polymer chains to the aggregates. To keep computation times within reasonable limits, most calculations are done on aggregates of 250 chains of 1000 segments each.

Aggregates of Monodisperse Homopolymer. As a first example we will investigate spherical aggregates of monodisperse 1000-mers in a bad solvent ($\chi = 1.0$). The self-consistent potentials and segment density profiles have been obtained for a total of 250 chains in a spherical lattice with 100 layers. The volume fractions in the interior of the particle and in the solution are of course equal to the two binodal ϕ values for the two coexisting phases at $\chi = 1.0$ as predicted by Flory's model for a 1000-mer. Figure 2a shows the total segment density profiles, $\phi(z)$, of the 1000-mer and the monomeric solvent as a function of the distance to the center of the particle. For the χ value chosen we still have about 30% (v/v) solvent in the interior of the particle. The segment density profile of the 1000-mer drops sharply for $z > 42$, forming an interface with a thickness of about 10 layers. The particle diameter in this case is about 90 layers. Taking a typical value of 0.4 nm for the layer thickness, this would correspond to about 36 nm. The interfacial region then has a thickness of about 4 nm which is roughly 20% of the particle radius. We define the interfacial region as the area where the density of solvent is more than 0.1% higher than inside the bulk of the particle and more than 0.1% lower than in the solution.

In a homogeneous amorphous polymer solution, every segment of the chain attributes, independent of its position in the lattice, the same contribution ($\phi(z,s) = \sum_s \phi(z,s)/r = \phi(z)/r$) to the overall density profile of the polymer. In the presence of an interface this will no longer be true. At the interface with the solvent, the distribution of chains over all possible conformations will be different from that in the interior of the particle. If the particle radius is large enough compared to the chain's radius of gyration, the conformational distribution of chains at the center of the particle can be expected to equal those of a homogeneous melt. Near or at the interface the contribution of individual segments to the overall profile depends on the position of the segment in the chain. In Figure 2b the individual segment density profiles scaled by the chain length, $r\phi(z,s)$, of some segments are shown. Because the chains are symmetrical, segments with a ranking number s higher than 500 have a profile equal to the corresponding segment $r - s + 1$ below 500, e.g., the profile of segment 1000 equals the one of segment 1. Therefore, in the case of chain symmetry, the profiles for segments with a ranking number higher than $r/2$ are left out. From Figure 2b it can be concluded that the end segments are preferentially located at the exterior side of the interface. Hence, the outer part of the particle interface is made up preferentially of chain ends resembling short hairs. About 34.4% of the

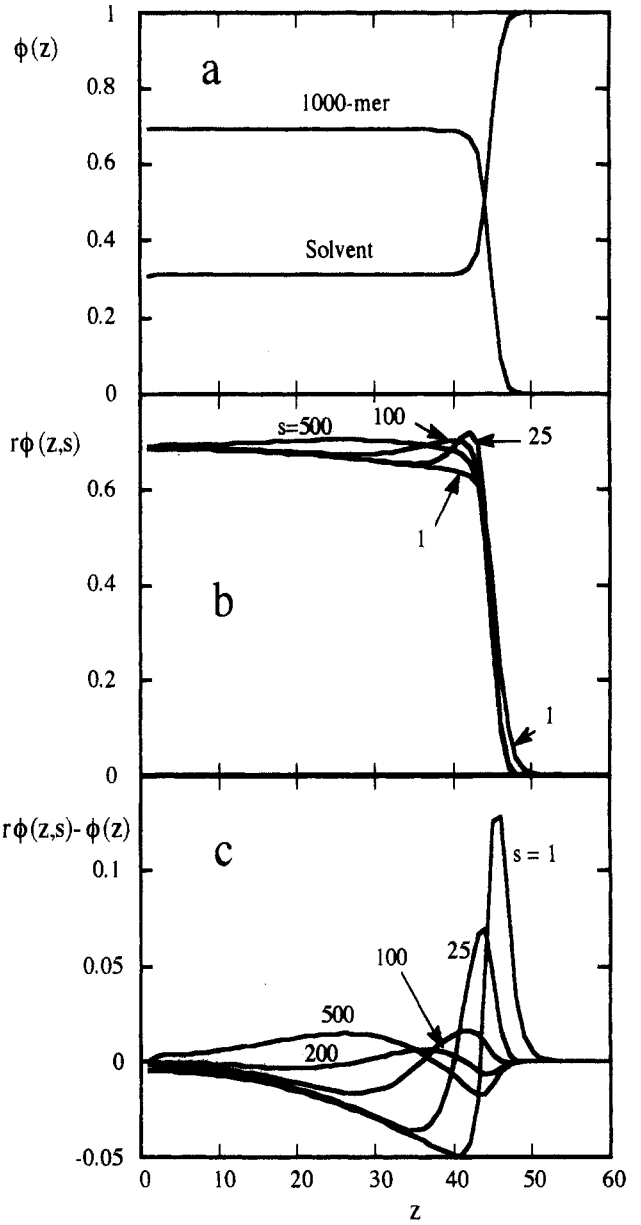

Figure 2. (a) Overall segment density profiles of a spherical aggregate of 1000-mers in a monomeric solvent. (b) Density profiles $r\phi(z,s)$ of individual segments (indicated). (c) Difference between the density profiles of individual segments (indicated) and the density profile of an average segment, $r\phi(z,s) - \phi(z)$. Other parameters: total number of segments of the 1000-mers in the system $nr = 250\,000$, $\chi = 1.0$, and $M = 100$.

segments at the very end of the chain (segments 1 and 1000) are found in the interfacial region of 10 layers, whereas of all segments only 31.5% are found in the interfacial region.

A different way to present these results in more detail is given in Figure 2c. In this figure the difference between the individual segment density profiles and the average segment density profile, $r\phi(z,s) - \phi(z)$, is shown for some segments at the chain end and at the chain center of the 1000-mer. It shows clearly that the end segments are preferentially located at the exterior side of the interface compared to the average segment and somewhat depleted from the interior side of the particle surface. Looking at Figure 2c, we also find this effect, although small, even for segment 100.

From a more detailed analysis it can be shown that the segments with a ranking number around $0.2r$ (or $0.8r$) have a distribution which is in all layers closest to the average

value. This special feature has also been reported by Scheutjens and Fleer.[13] For adsorbed homopolymers, they found values around $0.18r$ independent of the chain length. For the spherical particle, about 40% of the chain segments show an "end segment behavior"; i.e., they are depleted from the interior side of the interface to the exterior side. Segments showing a "middle segment behavior" are accumulated in the bulk phase of the particle and depleted from the interface with the solvent.

The effect of chain length on the total segment density of spherical homopolymer aggregates is shown in Figure 3a. At a constant total number of segments (nr = 250 000) we find that the total density profiles, i.e., $\phi(z)$, hardly change for chain lengths of 100 and longer. However, the deviation of the individual segments from the average segment density is largely dependent on the chain length. Figure 3 shows $r\phi(z,s) - \phi(z)$ for aggregates of three different chain lengths: 100 (b), 250 (c), and 500 (d). All other parameters are the same as for the 1000-mer in Figure 2. For longer chain lengths, the region in which a difference larger than, for instance, 0.001 is found increases. The width of this region indicates to what extend the interface affects the chain conformations, and it has a value of approximately 2 times the square root of the chain length ($2\sqrt{r}$). This means that particles with a total number of segments of 250 000 will not contain a homogeneous region at the particle center if the chain length is longer than 675. The width of the accumulation region of the end segments is nearly unaffected by the chain length because the chain lengths chosen are too long to provide enough chain ends to saturate the surface. In contrast, the width of the depletion region of the end segments increases strongly with increasing chain length. The radius of gyration of the chains at the interface will scale approximately as the square root of the chain length. Since the chain ends are preferentially located at the exterior side of the interface, we can expect the depletion zone to scale as twice the square root of the chain length to ensure a mass balancy. Also for the chain lengths shown in Figure 3 we find that segments with a ranking number around $s = 0.2r$ have a distribution closest to the average distribution. Thus, also for homopolymers in spherical aggregates there is hardly any influence of the chain length on this feature like in the case of homopolymer adsorption.

Varying the chain length at constant solvent quality (χ) and constant number of segments in the system has a large effect on the spatial position of the chain segments but hardly any effect on the overall density profile (Figure 3a). From changing the solvent quality we might expect a larger effect on the overall density profiles. If the contact energy between segments and solvent molecules increases as χ increases, it might be more favorable for the system to reduce the number of contacts between segments and monomers, i.e., to form a sharper interface, with the expense of loss of entropy. In Figure 4a overall segment density profiles are shown for 1000-mers in a spherical aggregate at a constant number of chains (n = 250) for various values of χ. The polymer volume fraction inside the particle increases with increasing χ as follows from Flory's theory for phase separation. Since the total amount of segments in the particle is constant (constant number of chains in the system), the particle radius decreases with increasing χ. In turn, improving the solvent quality, i.e., decreasing χ, lets the particle swell. For three solvent qualities, χ = 0.90, χ = 1.15, and χ = 1.25, the difference between the individual segment density profiles of some segments and the average segment density profiles is shown respectively in parts b–d of Figure 4. Only the shape of the accumulation region of the segments at the very end of the chains is affected by the solvent quality; all others

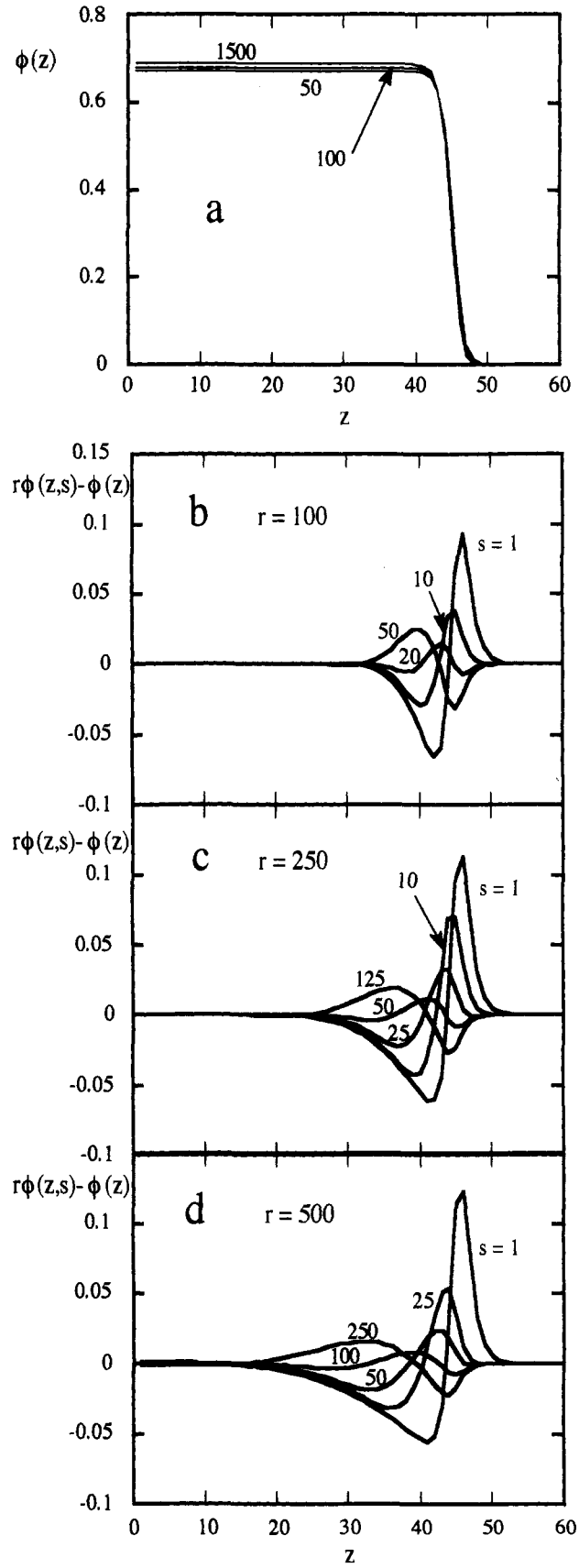

Figure 3. (a) Overall segment density profiles for spherical aggregates of 50-, 100-, and 1500-mers (indicated) having all the same amount of segments in the system nr = 250 000. Difference between the density profiles of individual segments (indicated) and the density profile of an average segment, $r\phi(z,s) - \phi(z)$, for a 100-mer (b), a 250-mer (c), and a 500-mer (d). All other parameters are the same as in Figure 2.

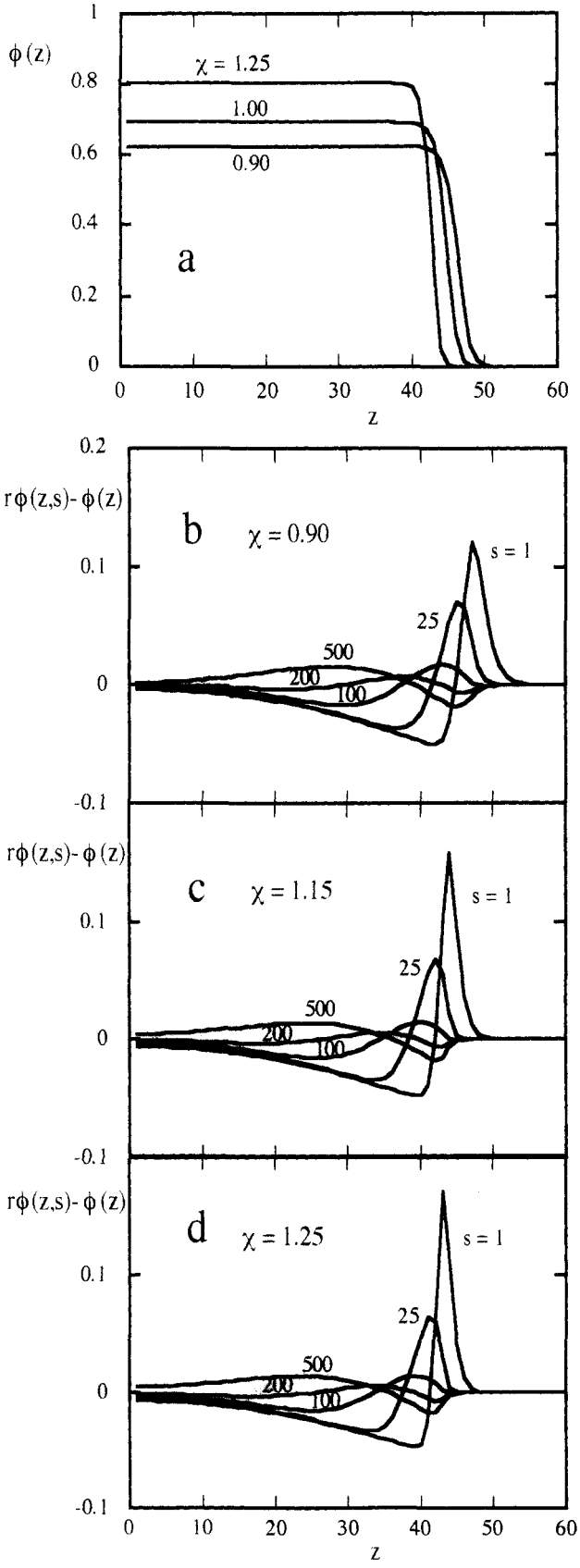

Figure 4. (a) Effect of the solvent quality χ (indicated) on the overall segment density profiles for a spherical aggregate of 1000-mers. Difference between the density profiles of individual segments (indicated) and the density profile of an average segment, $r\phi(z,s) - \phi(z)$, for $\chi = 0.9$ (b), $\chi = 1.15$ (c), and $\chi = 1.25$. (d) All other parameters are the same as in Figure 2.

are just shifted in correlation with the particle radius. The width of the accumulation region of the end segments at the exterior side of the interface decreases strongly with decreasing solvent quality. Hence, only the chain ends forming the short dangling hairs stretching out of the particle surface collapse with decreasing solvent quality. The percentage of segments at the very end of the chains located at the interfacial region decreases with decreasing solvent quality since the particle radius decreases. At $\chi = 0.90$, about 40.8% of the end segments are found at the interface compared to 38.1% of all segments. At $\chi = 1.25$ these numbers are respectively 23.7% and 20.5%. Thus, the ratio between the number of end segments and the total number of segments in the interfacial region changes from 1.07 for $\chi = 0.90$ up to 1.16 for $\chi = 1.25$. The decreasing solvent quality forces more chain ends to form dangling tails which are however in a more collapsed state.

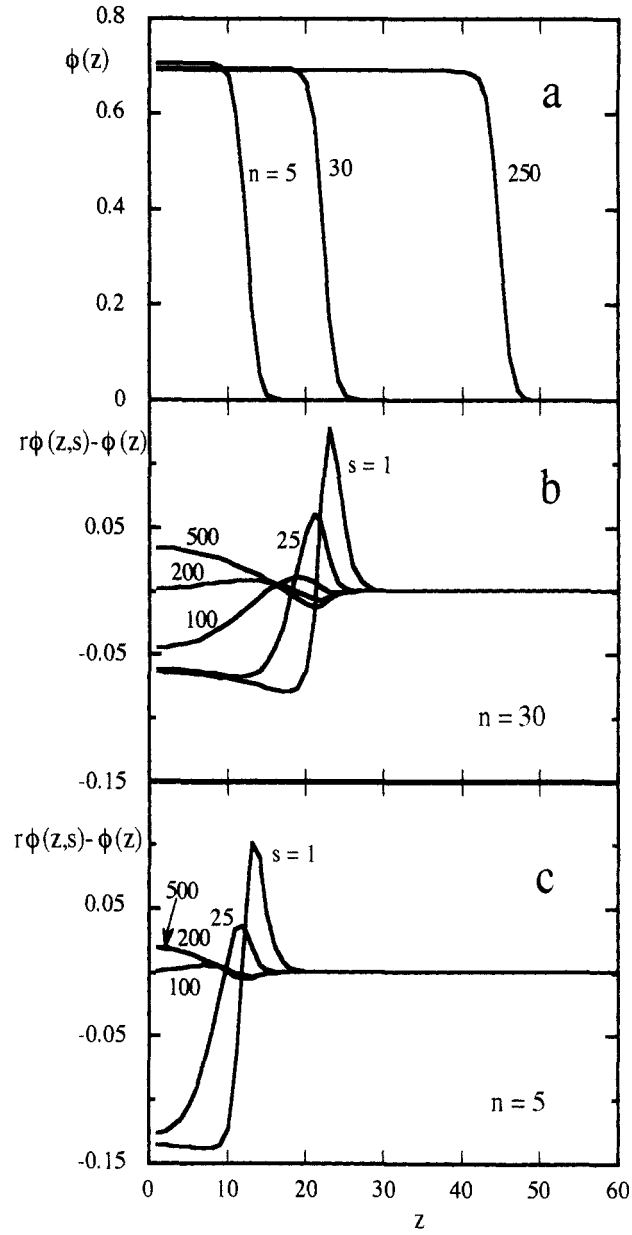

Figure 5. (a) Effect of the particle radius, i.e., the number of chains in the system (indicated) on the overall segment density profiles for spherical aggregates of 1000-mers. Difference between the density profiles of individual segments (indicated) and the density profile of an average segment, $r\phi(z,s) - \phi(z)$, for $n = 5$ (b) and $n = 30$ (c). All other parameters are the same as in Figure 2.

The effect of the particle radius, i.e., the number of chains, is shown in Figure 5 for aggregates of 1000-mers. At very low particle radius ($n = 5$) the number of segments showing an end segment behavior decreases drastically.

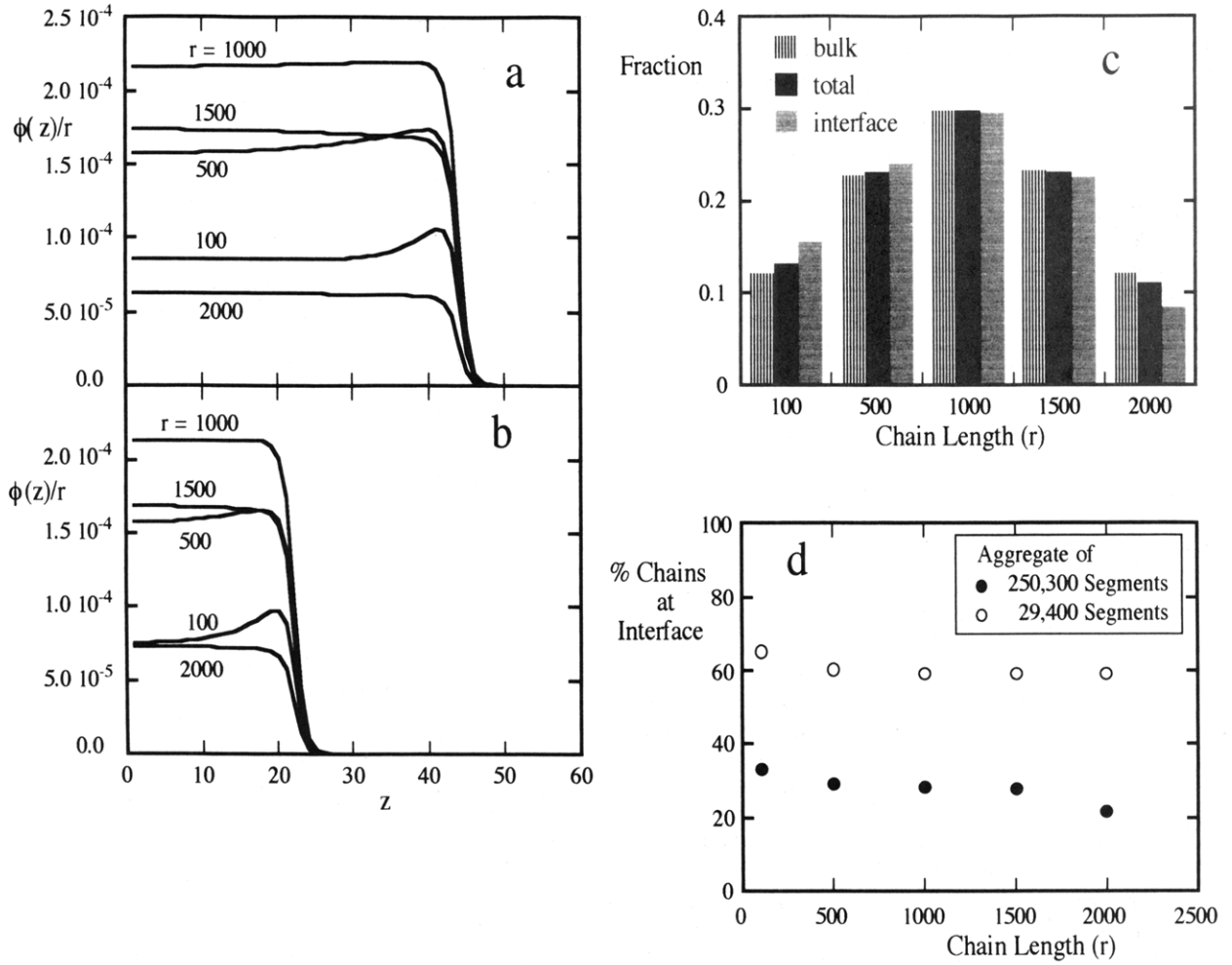

Figure 6. Segment density profiles of the average segment for every chain length (indicated) in a polydisperse polymer aggregate with a truncated normal distribution with $M_w/M_n = 1.34$. (a) Aggregate of 33 100-mers, 58 500-mers, 75 1000-mers, 58 1500-mers, and 28 2000-mers. (b) Aggregate of 4 100-mers, 7 500-mers, 9 1000-mers, 7 1500-mers, and 3 2000-mers. (c) Normalized chain length distributions of the total aggregate, of the bulk region of the aggregate, and of the interfacial region for the same aggregate as in (a). (d) Percentage of chains of every individual chain length fraction at the interface for both particles (indicated). All other parameters as in Figure 2.

For instance, at $n = 30$, segment 100 definitely shows an end segment behavior; i.e., it has a depletion zone at the particle center and accumulates at the interface. In contrast, at $n = 5$, no depletion zone is found for segment 100. In fact, the density profile of segment 100 is close to that of the average segment. The width of the interfacial region depends mainly on the solvent quality and hardly on the radius of the aggregate. For small aggregates compared to the chain length the interface will be saturated with chain ends which are shorter compared to the larger particles. Hence, for very small particles the fraction of segments showing an end segment behavior decreases drastically below the earlier found value of 40%.

Aggregates of Polydisperse Homopolymers. In most real polymers we are dealing with polydisperse polymeric materials. Especially the polymer chains in latex particles made by standard emulsion polymerization techniques are known to have a very broad chain length distribution. The effect of polydispersity on the distribution of the chains over the various possible conformations in spherical aggregates is discussed in this paragraph.

To mimic aggregates of polydisperse 1000-mers in a monomeric solvent, a mixture has been modeled of 33 100-mers, 58 500-mers, 75 1000-mers, 58 1500-mers, and 28 2000-mers. The total number of segments contained in the particle (nr) equals 250 300 as for the monodisperse 1000-mer aggregate of Figure 2. The polydisperse mixture has a normal chain length distribution with $M_w/M_n = 1.34$ truncated at higher chain lengths. The volume fraction profiles of the average segment, $\phi(z)/r_i$, for every chain length r_i in the aggregate are given in Figure 6a. It can be seen that near the interface with the solvent the shorter chains slightly accumulate. This should be expected since the loss of entropy due to the location at the interface is less for the shorter chains than for the longer chains. For this aggregate Figure 6c shows the normalized chain length distributions of the total aggregate, of the bulk region of the aggregate, and of the interfacial region. The width of the interfacial region is defined in the same way as has been done for the calculation of the fraction of end segments at the interface. The absolute number of chains in the interfacial region as well as in the bulk region cannot be calculated since there are chains which have parts in the bulk region and other parts in the interfacial region. We can however define the number of equivalent chains for a region, being the number of segments of those chains divided by the chain length. The normalized chain length distribution function at chain length r will then be defined by the number of equivalent chains of length r, $n(r)$, divided by the total number of chains n ($=\sum n(r)$). Figure 6c clearly shows the partitioning within the aggregate of the polydisperse polymer material over the bulk region and the interfacial region of the aggregate. The accumulation of segments of shorter chains at the interface can also be

observed for very small particle as shown in Figure 6b for a truncated normal distribution of chain lengths with $M_w/M_n = 1.34$ and a total number of segments equal to 29 400. In this case the numbers are 4 100-mers, 7 500-mers, 9 1000-mers, 7 1500-mers, and 3 2000-mers. There is however an interesting difference between the partitioning in very small particles and in particles of moderate size. To show this, the percentage of chains at the interface for every individual chain length fraction is given in Figure 6d for both particles. Of course, the fractions of chains at the interface are very high for the extremely small particle because of the larger surface to volume ratio. In total 59.4% of the segments are found at the interface of the very small particle compared to 26.6% in the case of the moderately sized particle. In the small particle the radius of gyration ($\sqrt{r}$) of the chains with more than 525 segments is already larger than the particle radius. This means that these longer chains can hardly be depleted from the interfacial region without greater losses of entropy. Therefore the fraction of equivalent chains at the interfacial region is constant for chain lengths above 525 and is just slightly below the overall fraction of equivalent chains at the interface (59% versus 59.4%). Only an accumulation of the shorter chains at the interface is observed. In the moderately sized particle even the radius of gyration of the 2000-mers is below the particle radius. Thus in this case the shorter chain lengths can deplete the longer chains from the interface and we do not find a constant fraction of equivalent chains at the interface for the higher chain lengths. In a future paper[19] we will be dealing with the effects of the polydispersity of chains on polymer aggregates in more detail.

Effect of Lyophilic Groups at the Chain End. As already discussed in the Introduction, the presence of lyophilic or even charged groups in the chains is assumed to have a large effect on the orientation of the chain ends and therefore on the film formation of some latices. In this section we will present results on the orientation of chains in spherical aggregates depending on the presence of one or more lyophilic groups in the chain.

As a first example we will present results of 1000-mers, with the first segment being lyophilic in a spherical aggregate of 250 chains. In the following we will denote lyophilic segments with A, lyophobic segments with B, and solvent monomers with O. The composition of the above-mentioned 1000-mer can then be described as A_1B_{999}. The degree of lyophilicity of the A segment is governed by the Flory–Huggins interaction parameter χ_{AO} between A and the solvent monomers O but also by the interaction parameter χ_{AB} between the lyophilic segment A and the lyophobic segment B. The more negative χ_{AO} gets, the more attractive the interaction between the A segments and the solvent monomers O becomes and the more lyophilic the A segments will be. Parts a–c of Figure 7 show the difference between the segment density profiles of some individual chain segments (indicated) and the density profile of an average segment at various degrees of lyophilicity (i.e., χ_{AO}) and repulsive interaction between the lyophilic and the lyophobic segments (i.e, χ_{AB}). As could be expected, the accumulation of the lyophilic segment ($s = 1$) at the interface increases with increasing attraction to the solvent (decreasing χ_{AO}) and increasing repulsion to the lyophobic segments (increasing χ_{AB}). For the percentage of lyophilic end segments at the interface we find the same effects; it ranges from 44% ($\chi_{AO} = -0.1$; $\chi_{AB} = 1.0$) to 46% ($\chi_{AO} = -0.5$; $\chi_{AB} = 1.0$) and even up to 53% ($\chi_{AO} = -0.5$; $\chi_{AB} = 2.0$). It is interesting to note that the percentage of

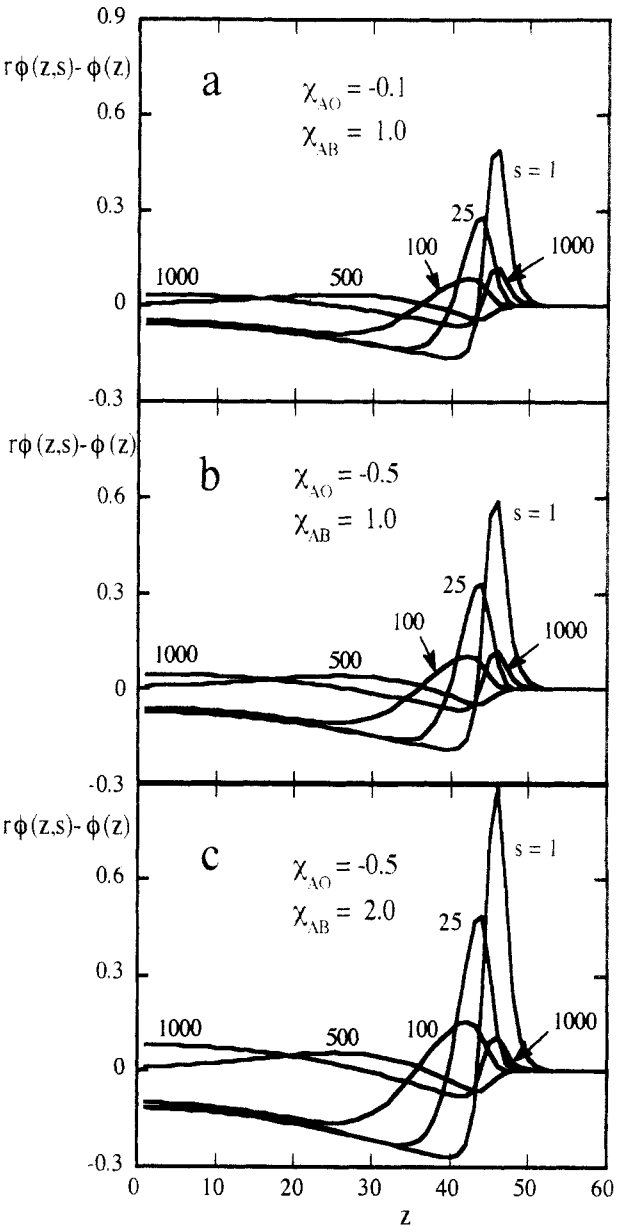

Figure 7. Effect of one lyophilic end segment per chain. Difference between the density profiles of individual segments (indicated) and the density profile of an average segment, $r\phi(z,s) - \phi(z)$, for aggregates of A_1B_{999} polymers, with A being the lyophilic segment and B being the lyophobic segments in an O solvent ($\chi_{BO} = 1.0$) at various interaction parameters χ_{AO} and χ_{AB} (indicated).

lyophobic end segments (other chain end) located at the interface remains about 33%. This value equals that of the end segments of the homopolymer with 1000 segments (Figure 2). However, it should be noticed that the lyophobic chain end shows a second accumulation region at the center of the particle. The aggregate can be subdivided into three regions: (1) the outermost shell representing the interfacial region containing a high accumulation of the lyophilic chain ends and an accumulation of the lyophobic chain end as in the case of pure homopolymer; (2) a region at the inner side of the surface containing an accumulation of middle segments, a strong depletion of the lyophilic chain ends and the lyophobic chain ends; (3) a region near the particle center which contains an accumulation of the lyophobic chain ends. The third region does not occur for pure homopolymers (see Figure 2). Because of the very high accumulation of lyophilic chain ends at the interface, the middle segments are much more strongly depleted from this region than in

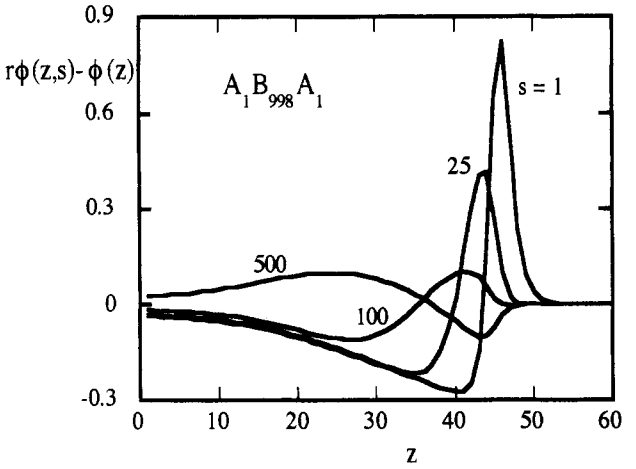

Figure 8. Effect of two lyophilic end groups. Difference between the density profiles of individual segments (indicated) and the density profile of an average segment, $r\phi(z,s) - \phi(z)$, of a spherical aggregate of 1000-mers with a lyophilic group at both chain ends, $A_1B_{998}A_1$. Other parameters: $\chi_{AO} = -0.5$, $\chi_{AB} = 1.0$, $\chi_{BO} = 1.0$.

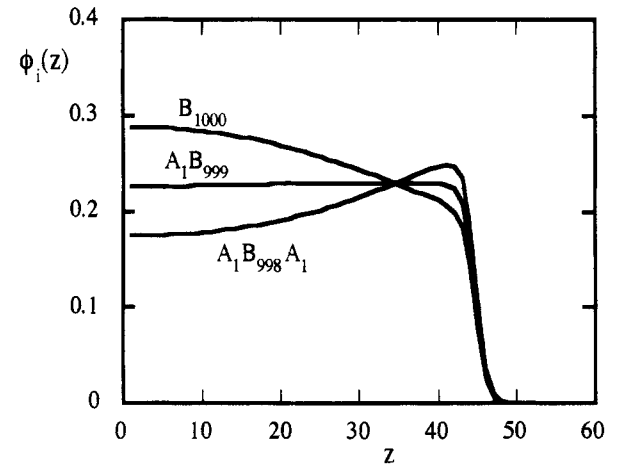

Figure 9. Segment density profiles for every chain type (indicated) for a spherical aggregate of a mixture of 83 1000-mers with no lyophilic groups (B_{1000}), 83 1000-mers with a lyophilic group at one chain end (A_1B_{999}), and 83 1000-mers with a lyophilic group at both chain ends ($A_1B_{998}A_1$). Other parameters are the same as in Figure 8.

the case of the pure homopolymer aggregates (note the difference of the y-axis scale between Figures 2c and 7). Due to the connection with both chain ends, the middle part of the chains then has to be accumulated more strongly next to the interface. This in turn forces the lyophobic chain ends to be depleted from this region more strongly as in the case of pure homopolymers, resulting in an accumulation in the central part of the aggregate.

Figure 8 shows the difference between the density profiles of individual segments and the average segment for a homopolymer with lyophilic groups at both chain ends, $A_1B_{998}A_1$. As could be expected we obtain the same type of profiles as for an aggregate of pure homopolymers. However, the degree of accumulation/depletion is much larger due to the attractive forces between the lyophilic segments and the solvent and in addition the repulsive forces between the lyophilic and the lyophobic segments.

It is interesting to investigate the aggregation from solution of a mixture of homopolymers bearing one, two, and no lyophilic end groups. Figure 9 shows the total density profiles of the chain types in the aggregate. In total the mixture contains 83 chains B_{1000}, 83 chains A_1B_{999}, and 83 chains $A_1B_{998}A_1$. A clear segregation within the particle of the three chain types is found. The chains

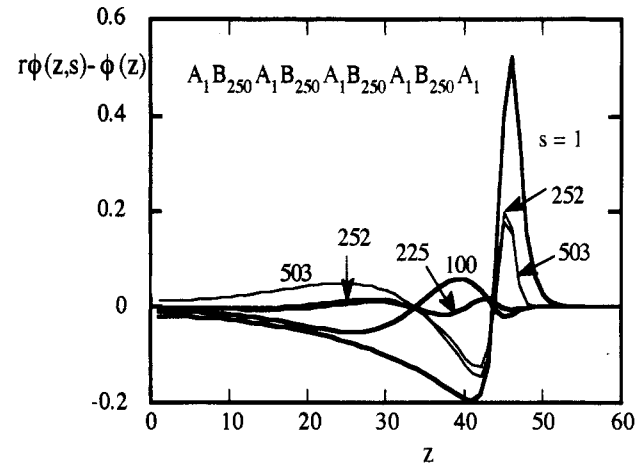

Figure 10. Effect of evenly distributed lyophilic groups. Difference between the density profiles of individual segments (indicated) and the density profile of an average segment is shown for an aggregate of $A_1B_{250}A_1B_{250}A_1B_{250}A_1B_{250}A_1$ polymers, with A being the lyophilic segment and B being the lyophobic segment. All parameters are the same as in Figure 8.

being able to compensate best for the loss of entropy due to the interface are accumulated at the interface, i.e., the chains with two lyophilic end groups. The pure homopolymers with no lyophilic end groups are strongly depleted from the interfacial region since they have the smallest energetic compensation for the loss of entropy. The profile of the homopolymer with one lyophilic end group is hardly affected by the presence of the other two chain types.

Effect of Lyophilic Groups Evenly Distributed over the Chain. To show the effect of lyophilic groups distributed evenly over the entire chain, we have calculated as an example spherical aggregates of the following polymer structure: $A_1B_{250}A_1B_{250}A_1B_{250}A_1B_{250}A_1$. Again, A is a lyophilic segment and B is a lyophobic segment ($\chi_{AO} = -0.5$, $\chi_{AB} = 1.0$, and $\chi_{BO} = 1.0$). Figure 10 shows the difference density profiles between individual segments and the average segment. For the segments at the very ends of the chain we find the same type of profile as for the $A_1B_{998}A_1$ polymers but the degree of accumulation/depletion is lower. This is due to the additional accumulation of the chain parts surrounding the lyophilic segments in the middle of the chain forming short loops at the surface. Note that the degree of accumulation/depletion of lyophilic "middle groups" seems to be rather independent of its actual position in the chain (compare segment 252 with segment 503).

IV. Conclusions

In this work we have applied the self-consistent mean-field lattice model of Scheutjens and Fleer[12-14] in a multicomponent version[16] to the description of spherical aggregates of homopolymers with and without lyophilic end groups. Since the model of Scheutjens and Fleer makes no a priori assumptions about the conformations of the chains in the lattice, it has shown to be a valuable model to obtain detailed information on the inner and surface fine structure of dispersed polymer particles. It must be pointed out that this theory is an equilibrium model. By applying the model to polymer aggregates, we will find the equilibrium distribution of chains within the particles. Real latex particles may however be far from equilibrium.

For particles of pure homopolymers without lyophilic end groups it is found that the chain ends have a slight preference for the particle surface. The segment density

profiles drop sharply at the interface which has a thickness of roughly 10 lattice layers corresponding typically to about 4 nm. The outer part of the particle interface is made up preferentially of chain ends resembling short hairs. The chain segments can be divided into two groups: segments showing an end segment behavior (i.e., they are accumulated at the interface) and segments showing a middle segment behavior (i.e., they are depleted from the interface). For particles large enough compared to the chain dimensions, about 40% of the segments show an end segment behavior. The width of the region perpendicular to the surface in which a difference between the spatial distribution of the individual segments and the average segment is found is approximately 2 times the square root of the chain length. Depending on the solvent quality, particles are found to swell or shrink according to Flory's phase separation theory. The width of the accumulation region of the end segments at the exterior side of the interface decreases strongly with decreasing solvent quality. Thus, the short dangling hairs stretching out of the particle surface collapse with decreasing solvent quality.

For particles of polydisperse pure homopolymers without lyophilic groups it is found that the shorter chains slightly accumulate at the interface. This should be expected since the loss of entropy due to the location at the interface is less for the shorter chains than for the longer chains.

For particles of homopolymers with one lyophilic group at one chain end we find that the accumulation of this chain end at the interface increases with increasing attraction between the lyophilic segment and the solvent and with increasing repulsion of the lyophilic segment to the lyophobic segment. The accumulation of the lyophilic chain end is much stronger than in the case of pure homopolymers. For the interaction parameters used, up to 53% of the lyophilic chain ends were found at the interface. Particles of homopolymers with two lyophilic chain ends show a very strong accumulation of both chain ends at the surface.

Interesting is the large fractionation within the particle for the case of aggregates of a mixture of homopolymers with one, two, and no lyophilic groups. The pure homopolymers are strongly depleted to the particle inner bulk phase, whereas the chains with two lyophilic end groups are highly accumulated at the particle surface.

Acknowledgment. We thank Dr. J. Rieger of the Kunststofflaboratorium, BASF Aktiengesellschaft, for his valuable suggestions and interest in this work.

List of Symbols

$g_i(z,s)$	unconditional weighting factor to find segment s of a molecule of type i in layer z
$g_i(z,s\|1)$	conditional weighting factor to find segment s of the chain part from segment 1 up to segment s of a molecule of type i in layer z
$g_i(z,s\|r_i)$	conditional weighting factor to find segment s of the chain part from segment s up to the last segment r_i of a molecule of type i in layer z
$g_x(z)$	unconditional weighting factor to find a segment of type x in layer z
i	index of molecule type
k	Boltzmann's constant
l_0	thickness of a layer
n_i	number of molecules of type i in the M layers
r_i	chain length of molecules of type i expressed in number of segments
s	index of segment ranking number
$u'(z)$	hard-core potential in layer z
$u_x(z)$	potential of a segment of type x in layer z
$u_x^{\text{int}}(z)$	energetic part of the potential of a segment of type x in layer z
x	index of segment type
y	index of segment type
z	index of layer ranking number
C_i	normalization constant for the segment densities of molecules of type i
$L(z)$	volume of layer z
M	total number of layers of the lattice
M_n	number-average molecular weight
M_w	weight-average molecular weight
$S(z)$	outer surface area of layer z
T	temperature
V	total volume of the M layers
Z	coordination number of the lattice
$\phi_i(z)$	volume fraction of all segments of molecules of type i in layer z
$\phi_i(z,s)$	volume fraction of only segment s of molecules of type i in layer z
$\phi_x(z)$	volume fraction of segments of type x in layer z
$\langle\phi_x(z)\rangle$	average volume fraction of segments of type x a segment has in layer z
λ_0	fraction of nearest neighbors a site in a planar lattice has in the same layer
λ_1	fraction of nearest neighbors a site in a planar lattice has in an adjacent layer
$\lambda(z',z)$	a priori transition probability to make a random-walk step from layer z to layer z'
χ_{xy}	Flory–Huggins interaction parameter between segment types x and y

References and Notes

(1) Hahn, K.; Ley, G.; Schuller, H.; Oberthür, R. *Colloid Polym. Sci.* **1986**, *264*, 1092.
(2) Hahn, K.; Ley, G.; Oberthür, R. *Colloid Polym. Sci.* **1988**, *266*, 631.
(3) Linné, M. A.; Klein, A.; Miller, G. A.; Sperling, L. H. *J. Macromol. Sci., Phys.* **1988**, *B27* (2 & 3), 217.
(4) Yoo, J. N.; Sperling, L. H.; Glinka, C. J.; Klein, A. *Macromolecules* **1991**, *24*, 2868.
(5) van den Hul, H. J.; Vanderhoff, J. W. *Br. Polym. J.* **1970**, *2*, 121.
(6) de Gennes, P.-G. *J. Chem. Phys.* **1971**, *55*, 572.
(7) de Gennes, P.-G. *C. R. Acad. Sci. Paris* **1980**, *B291*, 219.
(8) Mansfield, K. F.; Theodorou, D. N. *Macromolecules* **1989**, *22*, 3143.
(9) Kumar, S. K.; Vacatello, M.; Yoon, D. Y. *Macromolecules* **1990**, *23*, 2189.
(10) Bitsanis, I.; Hadziioannou, G. *J. Chem. Phys.* **1990**, *92*, 3827.
(11) Madden, W. G. *J. Chem. Phys.* **1987**, *87*, 1405.
(12) Scheutjens, J. M. H. M.; Fleer, G. J. *J. Phys. Chem.* **1979**, *83*, 1619.
(13) Scheutjens, J. M. H. M.; Fleer, G. J. *J. Phys. Chem.* **1980**, *84*, 179.
(14) Scheutjens, J. M. H. M.; Fleer, G. J. *Macromolecules* **1985**, *18*, 1882.
(15) Theodorou, D. N. *Macromolecules* **1989**, *22*, 4578.
(16) Evers, O. A.; Scheutjens, J. M. H. M.; Fleer, G. J. *Macromolecules* **1990**, *23*, 5221.
(17) van Lent, B.; Scheutjens, J. M. H. M. *Macromolecules* **1989**, *22*, 1931.
(18) Marqusee, J. A.; Dill, K. A. *J. Chem. Phys.* **1986**, *85*, 434.
(19) Evers, O. A.; Ley, G.; Hädicke, E., to be published.